Molecular clamp stabilised Spike protein for protection against SARS-CoV-2

Daniel Watterson
University of Queensland https://orcid.org/0000-0001-5957-2853
Danushka Wijesundara
University of Queensland
Naphak Modhiran
University of Queensland
Francesca Mordant
University of Melbourne https://orcid.org/0000-0002-3754-2642
Zheyi Li
Australian National University
Michael Avumegah
The University of Queensland https://orcid.org/0000-0003-2325-2238
Christopher McMillan
The University of Queensland https://orcid.org/0000-0002-5316-0986
Julia Lackenby
The University of Queensland
Kate Guilfoyle
Viroclinics Xplore
Geert van Amerongen
ViroClinics DDL
Koert Stittelaar
Viroclinics Xplore
Stacey Cheung
The University of Queensland
Summa Bibby
The University of Queensland
Mallory Daleris
The University of Queensland
Kym Hoger
The University of Queensland
Marianne Gillard
The University of Queensland
Eve Radunz
The University of Queensland https://orcid.org/0000-0002-4734-2898
Martina Jones
The University of Queensland https://orcid.org/0000-0002-5154-6017
Karen Hughes
The University of Queensland
Ben Hughes
The University of Queensland
Justin Goh
The University of Queensland https://orcid.org/0000-0002-4982-193X
David Edwards
The University of Queensland
Judith Scoble
CSIRO

Lesley Pearce
CSIRO
Lukasz Kowalczyk
CSIRO
Tram Phan
CSIRO
Mylinh La
CSIRO
Louis Lu
CSIRO
Tam Pham
CSIRO
Qi Zhou
CSIRO
David Brockman
TetraQ
Sherry Morgan
StageBio
Cora Lau
The University of Queensland
Mai Tran
TetraQ
Peter Tapley
TetraQ
Fernando Villalon Letelier
University of Melbourne
James Barnes
WHO-CC
Andrew Young
The University of Queensland
Noushin Jaberolansar
The University of Queensland
Connor Scott
University of Queensland https://orcid.org/0000-0001-9535-1863
Ariel Isaacs
University of Queensland https://orcid.org/0000-0002-8499-3083
Alberto Amarilla
University of Queensland
Alexander Khromykh
University of Queensland
Patrick Reading
University of Melbourne
Charani Ranasinghe
Australian National University
Kanta Subbarao
WHO Collaborating Centre for Reference and Research on Influenza https://orcid.org/0000-0003-1713-3056
Trent Munro
The University of Queensland https://orcid.org/0000-0003-1987-2020
Paul Young
University of Queensland
Keith Chappell (k.chappell@uq.edu.au)
University of Queensland

Article

Keywords: Sclamp, Rational Antigen Design, Manufacturability, Vaccine Efficacy, Syrian Hamsters,

Posted Date: October 1st, 2020

DOI: https://doi.org/10.21203/rs.3.rs-68892/v1

Abstract

Efforts to develop and deploy effective vaccines against Severe Acute Respiratory Syndrome Coronavirus 2 (SARS-CoV-2) continue at pace with more than 30 candidate vaccines now in clinical evaluation. Here we describe the preclinical development of an adjuvanted, prefusion-stabilised Spike (S) protein "Sclamp" subunit vaccine, from rational antigen design through to assessing manufacturability and vaccine efficacy. In mice, the vaccine candidate elicits high levels of neutralising antibodies to epitopes both within and outside the receptor binding domain (RBD) of S, as well as broadly reactive and polyfunctional S-specific CD4+ and cytotoxic CD8+ T cells. We also show protection in Syrian hamsters, which has emerged as a robust animal model for pulmonary SARS-CoV-2 infection. No evidence of vaccine enhanced disease was observed in animal challenge studies and pre-clinical safety was further demonstrated in a GLP toxicology study in rats. The Sclamp vaccine candidate is currently progressing rapidly through clinical evaluation in parallel with large-scale manufacture for pivotal efficacy trials and potential widespread distribution.

Introduction

The scientific community, including critical industry and academic partnerships, have embarked on an unprecedented race to develop and produce effective COVID-19 vaccine(s) for global use[1]. Several recent reports validate the SARS-CoV-2 Spike (S) protein as a promising target for COVID-19 vaccine development[2–5]. However, these approaches utilise platforms based on nucleic acids, viral vectors or insect cell production systems which could face challenges during large-scale manufacture and distribution.

Our candidate vaccine, SARS-CoV-2 Sclamp, consists of the recombinant viral S glycoprotein stabilised in its prefusion trimeric form, through the incorporation of a "molecular clamp" stabilisation domain, and produced in mammalian cells (Chinese Hamster Ovary)[6]. Stabilisation of the prefusion antigen is a major goal of next generation vaccines that target enveloped viruses. This approach ensures that vaccines elicit the production of specific antibodies that recognise a wider array of conserved epitopes, including conformational epitopes, that are displayed on the virion surface[7,8].

Herein we describe the rapid development of the Sclamp vaccine, including antigen design and characterisation, process optimisation, and animal immunogenicity, safety and efficacy studies.

Accelerated development of a highly expressed prefusion conformed Sclamp

The virus genomic sequence first became available on the 12th of January, 2020[9] and we immediately commenced development of a candidate subunit vaccine utilising the molecular clamp platform (a timeline of research and development and an overview of the molecular clamp platform are included in Extended Data Figs. 1 and 2). Within 34 days, we had expressed and screened > 200 antigens incorporating truncations and modifications at key sites within the coding sequence of the S glycoprotein to identify a lead candidate, with high expression and affinity to S-specific monoclonal antibody (mAb), CR3022[10] (Fig. 1A-D and Supplementary Table 1). The optimal lead construct incorporated the S protein native signal peptide, replacement of aa680-690 with a Glycine linker (GSG), truncation at aa1204 and followed by the molecular clamp coding sequence. This construct was termed M1GSG (Supplementary Fig. 1 and Supplementary Table 1).

We solved the 5 Å resolution structure of this Sclamp construct in the closed trimeric prefusion conformation by Cryo-TEM (Fig. 1E). Using size-exclusion high-performance liquid chromatography (SE-HPLC) and TEM, we demonstrated that Sclamp can also adopt the open prefusion conformation[11], and that the antigen exists in an equilibrium between these two conformations, with exposure to varying pH or temperature driving transition between the open and closed forms (Extended Data Figs. 3 and 4).

Transient gene expression in CHO cells was initially utilised to allow rapid screening of antigen design panels with CHO stable cell lines being established following lead candidate selection. Transitioning to CHO stable pools and using a fed batch bioprocess resulted in increased expression yields in shaker flasks of 100–150 mg/L and in bioreactors up to 500 mg/L (Fig. 1F). This level of mammalian cell-based protein expression is an order of magnitude higher than previously reported for an "optimised" S protein construct[12] and has the potential to generate many millions of doses per bioreactor run using industry standard mammalian cell bioprocessing facilities.

We utilised several, patient derived, SARS-CoV-2 cross-reactive mAbs (CR3022[10], S309[13] and CB6[14]), to demonstrate high affinity binding to the Sclamp protein and hence conformational integrity (S309 kD = 0.08 nM; CB6 kD = 0.15 nM). We also confirmed that the trimeric conformation and antibody recognition of Sclamp are retained, even after prolonged exposure to heat stress (Fig. 1H and Extended Data Fig. 5), indicating that a long shelf-life may be achievable without the need for low temperature, frozen storage in the optimised vaccine formulation.

MF59C.1-adjuvanted Sclamp vaccination elicited effective neutralising antibodies against SARS-CoV-2

Purified protein-based vaccines require adjuvant co-administration to enhance immunogenicity and to reduce the total amount of antigen required to provide protective immunity[15]. The squalene-oil-in-water adjuvant MF59C.1® (Seqirus) was selected for use with our vaccine due to its well-established safety record and its ability to stimulate a balanced T helper (Th1/Th2) cell response[16]. Alhydrogel was included as a comparator adjuvant[17,18]. BALB/c mice received intramuscular (IM) injections of PBS (placebo) or two doses of Sclamp with or without Alhydrogel or MF59C.1 (Fig. 2A). Vaccinated mice developed a robust antigen-specific IgG response after a single dose with either adjuvant and this was boosted following the second dose (Fig. 2B).

All mice receiving two doses of Sclamp with either Alhydrogel or MF59C.1 produced a strong neutralising antibody response as assessed in a microneutralisation (MN) assay (Fig. 2C). Virus neutralisation, as assessed by a plaque reduction neutralisation test ($PRNT_{50}$) assay, was observed equally for both 614D and 614G SARS-CoV-2 variants in serum, and also in bronchoalveolar lavage (BAL) samples (Fig. 2F and Supplementary Fig. 2). A subsequent assay was conducted that included a WHO recommended reference serum (NIBSC code 20:130)[19] to allow benchmarking of the neutralising titre to other platforms. In this assay, sera from mice vaccinated with MF59C.1-adjuvanted Sclamp neutralised SARS-CoV-2 with an ~ 2-fold higher geometric mean titre (GMT) compared to the reference serum (Extended Data Fig. 6A).

Using a depletion ELISA to block the clamp tag-, RBD- and Sclamp-specific antibodies, the relative specificity of the antibody response to the clamp trimerisation tag, RBD subdomain and SARS-CoV-2 S ectodomain, was assessed in the initial immunogenicity study (Fig. 2D/G), and in a second immunogenicity study designed to assess post-formulation stability (Extended Data Fig. 6). In both studies, we found that on average 70–76% of antibodies were specific to the ectodomain, of which roughly half were directed to the RBD and half to other epitopes within the ectodomain. Interestingly, while the relative percentage of the immune response to the clamp itself varied between individual animals, this 'off target' response was not associated with a decrease in either the overall response to the ectodomain or the MN_{50} titres (Extended Data Figs. 6C, 7A and 7B). RBD-specific antibodies contributed, on average, ~ 50% of MN activity, with a high degree of inter-animal variation (SD = 27.9%). In comparison, MN activity was reduced by nearly 100% by the Sclamp depletion control (Fig. 2E/H). This finding indicates that antibodies to the RBD contribute substantially to MN activity, but that antibodies specific to S domains outside the RBD also make a significant contribution to overall neutralising activity. Notably, the S-specific IgG titre was a better correlate of MN activity compared to the RBD-specific IgG titre (R^2 fit = 0.77 and 0.22, respectively; Extended Data Fig. 7C and 7D).

MF59C.1-adjuvanted Sclamp vaccination elicited robust S-specific polyfunctional/cytotoxic $CD4^+$ and $CD8^+$ T cell immunity

We evaluated SARS-CoV-2 S-specific $CD4^+$ and $CD8^+$ T cell responses *in vivo* using a fluorescent target array (FTA) analysis and complementary intracellular cytokine staining (ICS) analysis to determine type 1 vs type 2 immunity[20,21]. For FTA analysis, mice were challenged with fluorescent-bar coded cells pulsed with peptide pools that collectively span the SARS-CoV-2 S_{1-1226} sequence (Fig. 3A and 3B). In this assay, up-regulation of CD69 on S peptide-pulsed $B220^+$ cells recovered from challenged mice indicates the presence of antigen-specific Th cell responses and the killing of cognate peptide-pulsed targets is a result of cytotoxic T lymphocyte (CTL) responses *in vivo*. Specifically, our findings revealed that Alhydrogel-adjuvanted vaccination was more effective in eliciting S-specific Th cell and CTL responses compared to Sclamp only and placebo control groups (Fig. 3C and Supplementary Tables 2–3) but MF59C.1-adjuvanted vaccination elicited the highest magnitude and the broadest S-specific Th cell and CTL responses *in vivo* (Fig. 3C and Supplementary Tables 1–2). This trend was evident for Th cell responses to $S_{185-362}$ (P2), $S_{353-530}$ (P3), $S_{521-698}$ (P4), $S_{689-886}$ (P5), $S_{857-1070}$ (P6), $S_{1041-1226}$ (P7), S_{16-554} (S1), $S_{673-1218}$ (S2), Peptivator (Miltenyi Biotec) and the S_{1-1226} (Total), but not for S_{1-194} (P1). CTL immunity followed a similar trend, but not with responses to P6 and P7.

Consistent with the FTA analysis, mice vaccinated with MF59C.1-adjuvanted Sclamp developed the highest number of S-specific $CD4^+$ or $CD8^+$ T cells that expressed mono- or poly-functional interferon (IFN)-γ, tumour necrosis factor (TNF)-α and/or interleukin (IL)-2 (Fig. 3D, and Supplementary Fig. 2 and Supplementary Tables 4–5). Furthermore, these mice developed higher numbers of IFN-γ^+, TNF-α^+ and/or IL-2^+ T cells compared to IL-4^+ and/or IL-13^+ counterparts (Fig. 3E).

Sclamp vaccination was safe and induced protection against pathogenic SARS-CoV-2 challenge

Given that the molecular clamp platform has not previously been used in humans, we conducted a repeat dose toxicity study in Sprague Dawley rats (data not shown). Three doses of MF59C.1-adjuvanted Sclamp at the maximum feasible dose administered by IM injection at two-week intervals, were well tolerated. Treatment-related observations were limited to the injection site and included mild inflammatory cell infiltration and minimal myodegeneration. No other adverse findings were observed.

To evaluate Sclamp-mediated protection and to investigate the possibility of vaccine-enhanced respiratory disease, we completed two studies in which hamsters were challenged with intranasal inoculation following either a single dose or a prime/boost vaccination regimen (Fig. 4 and

Extended Data Fig. 8), and one in ferrets following a similar inoculation and challenge regimen (Extended Data Fig. 9). In the hamster model, a single dose of MF59C.1-adjuvanted Sclamp resulted in a substantially reduced virus load in the lungs at day 4 post infection ($p < 0.001$), with 5/10 animals having undetectable levels of virus in the lungs (Extended Data Figure Fig. 8D). In the prime/boost study, administration of two doses of MF59C.1-adjuvanted Sclamp resulted in complete protection in the lungs for all but one animal at 4 days post infection. The two-dose regimen reduced viral $TCID_{50}$ titres in the nasal turbinates from 2.9×10^7 to 3.8×10^6, although this was not statistically significant (Fig. 4D). However, peak viral loads in daily throat swabs collected in both the single dose and prime/boost studies were significantly reduced compared to placebo controls (Fig. 4C and Extended Data Fig. 8C).

Histopathological assessment of placebo vaccinated hamsters at day 4 and at day 8 provides an interesting snapshot of disease, with inflammation primary confined to the upper respiratory tract and larger airways (trachea and bronchus) at day 4 but then proceeding to the smaller airways (bronchioles and alveoli) at day 8 and impacting a greater percentage of lung tissue, despite the apparent clearance of virus from the lung by this timepoint (Fig. 4 and Extended Data Fig. 8). Importantly, two doses of MF59C.1-adjuvanted Sclamp was found to be significantly protective against rhinitis, tracheitis and bronchitis at day 4, as well as bronchiolitis and alveolitis at day 8 (Fig. 4F and I and Extended Data Fig. 10). In addition two doses of MF59C.1-adjuvanted Sclamp significantly reduced the overall percentage of the lung affected at day 8 (Fig. 4H) and provided protection against peribrochial/pervascular cuffing, alveolar oedema and alveolar haemorrhage (Supplementary table 6). A single dose of MF59 adjuvanted Sclamp was also shown to provide a significant level of protection against bronchitis, bronchiolitis and alveolitis (Extended Data Fig. 9F).

In the ferret model of SARS-CoV-2 infection, viral replication was primarily restricted to the upper respiratory tract, with no virus isolated from lung tissue at day 4 post infection (Extended Data Fig. 10). While there was a tendency for reduced viral loads in daily nasal and throat swabs from animals receiving a single dose of MF59C.1-adjuvanted Sclamp, there was substantial inter-animal variation and consequently the differences were not statistically significant. Nonetheless, histopathological assessment of rhinitis demonstrated a significant reduction of inflammatory cells following MF59C.1-adjuvanted Sclamp vaccination ($p = 0.01$).

Discussion

Vaccine development in response to the COVID-19 pandemic has been unprecedented both in terms of speed and the diversity of the underlying technology platforms. These approaches have included inactivated viruses, nucleic acid-based vaccines, viral vectors and protein subunits[22]. While each of these platforms comes with its own strengths and limitations, this diversity should also increase the likelihood of success and allow for the selection of the optimal vaccine(s) to progress into wide-spread global use based on key parameters, including safety and efficacy[23].

Driven by the rationale that any improvement in protein yield directly translates into a future increase in dose availability, we dedicated considerable effort to the selection of an optimal candidate and development of a high-yielding and scalable bioprocess. The ability to manufacture at large-scale, ensuring consistent product quality, together with supply chain stability, will be a critical differentiator in achieving global vaccine supply[23].

In mice, vaccination with MF59C.1-adjuvanted Sclamp was found to elicit a robust humoral immune response that efficiently neutralised both the original SARS-CoV-2 strain and the D614G variant which has since become the dominant circulating strain. We confirmed that the vaccine elicited neutralising antibodies against a broad array of epitopes, including those both inside and outside the RBD. These findings provide confidence that the breadth of vaccine efficacy should extend to ‘drifted’ strains, and minimise the potential impact of the emergence of escape mutants[24].

A major issue in comparing results between vaccine platforms is that there is no standardised method for assessing virus neutralisation. To address this issue, WHO has recommended the use of a pooled convalescent patient reference serum (NIBSC code 20:130) until an international standard can be made available at the end of 2020[19]. Serum from mice that received two doses of MF59C.1-adjuvanted Sclamp was found to neutralise SARS-CoV-2 at twice the level of the reference serum. To our knowledge no other programs have reported neutralising titres relative to this reference serum. Therefore, this data provides a useful cross-platform comparator.

In addition to the humoral immune response, type 1 biased S-specific T cell immunity likely contributes to protection in convalescent COVID-19 patients[25]. Broadly-reactive and/or type 1 cytokine producing T cell responses are also characteristic of DNA, Adenovirus serotype 26 and chimpanzee Adenovirus vaccines that protected non-human primates against SARS-CoV-2 challenge and are in clinical development[2,4,5]. *In vivo* and *in vitro* T cell analyses in our study demonstrated that MF59C.1-adjuvanted Sclamp vaccination elicited a robust, broad and type 1 biased polyfunctional T cell response in mice, consistent with features of a T cell response that could contribute to protection against SARS-CoV-2.

Although non-human primates represent an attractive model for SARS-CoV-2 vaccine development[2–5], multiple studies[26–28] including our own suggest that the Syrian hamster provides an effective animal model to evaluate SARS-CoV-2 vaccine efficacy for the following reasons: 1) low dose (i.e. 10^2-10^3 $TCID_{50}$) i.n. administration of SARS-CoV-2 results in replication of infectious virus to high titres in the respiratory tract (lungs and nasal turbinates), 2) hamsters are permissive to communicable transmission[26], 3) hamsters can develop severe pneumonia and lung injury similar to COVID-19 patients[28], and 4) protection can be reproducibly evaluated based on infectious viral load rather than viral genomic copy levels[26–28].

A single dose of MF59C.1 adjuvanted Sclamp afforded a level of protection to hamsters from SARS-CoV-2 infection, with a significant decrease in viral replication, reduced lung inflammation and disease severity. Administration of two doses further improved lung protection in hamsters and suggested this protection may extend to the upper respiratory tract. These findings are in line with our mouse immunogenicity studies which demonstrated that a prime/boost strategy maximised the neutralising antibody response to SARS-CoV-2. Moreover, we demonstrated some evidence of protection in the ferret model, although ferrets were markedly less permissive to SARS-CoV-2 infection. Importantly, no evidence of vaccine-enhanced respiratory disease was observed in either hamsters or ferrets.

Overall, this work demonstrates the ability of MF59C.1 adjuvanted Sclamp to provide protection against SARS-CoV-2 infection and supports continued development and progression through human clinical trials. This candidate vaccine has significant advantages that make it well-suited to meet the global response to the COVID-19 pandemic, notably the well-established safety record for the use of subunit vaccines and the MF59C.1 adjuvant, and the compatibility of the manufacturing process with industry standard bioprocess facilities.

Declarations

Acknowledgements

This work was funded by the Coalition for Epidemic Preparedness Innovations (CEPI). We would like to thank Mike Whelan, Raafat Fahim and the rest of the project management team from CEPI for all their expert advice and guidance. Further funding support was provided by The Queensland State Government, The Medical Research Future Fund, The a2 Milk Company (Australia) Pty Ltd, The Golden Casket Foundation, The Bryan Foundation, Research Donation Generic, Royal Automobile Club of Queensland (RACQ), Liming International Pty Ltd, Research Donation Generic, Aurizon Operations Limited, NewCrest Mining Limited, Dr Jian Zhou Foundation, The Bowness Family Foundation, Glencore Australia Holdings Pty Limited, BHP Foundation, Paul Ramsay Foundation Limited, and others.

MF59C.1 adjuvant was provided by Seqirus and we would like to thank CSL and Seqirus for the assitance with manufacturing process development. We would like to thank Cytiva for their development of the custom immunoaffinity resin, Berly lights for assistance optimizing clonal cell line selection and Lonza and Thermofisher for the provision of CHO cell lines.

We would like to thank Christina Henderson for administrative coordination and The University of Queensland Legal, Finance and Communications teams. We would like to thank Virginia Nink and Nadia De Jager at the Queensland Brain Institute for their help with the flow cytometry. Antigen production was supported by the National Biologics Facility and Therapeutic Innovation Australia. We thank the facilities, and the scientific and technical assistance, of the Australian Microscopy & Microanalysis Research Facility at the Centre for Microscopy and Microanalysis and the Research Compute Centre, the University of Queensland, in particular the assistance of Drs Roger Wepf, Lou Brillault and Matthias Floetenmeyer. We thank Nvidia for the supply of a DGX workstation to aid computational analysis of cryo-EM data, and Michael Landsberg for assistance. We would like to thank NIBSC for the provision of the reference serum. We also thank Jake Carrol and the Research Computing Center at UQ for technical assistance.

KS is supported by NHMRC Investigator grant 1177174 and generous support of the Jack Ma Foundation and the a2 Milk Company. The Melbourne WHO Collaborating Centre for Reference and Research on Influenza is supported by the Australian Government Department of Health. SARS-CoV-2 isolates QLD02 and QLD935 were provided by Queensland Health Forensic & Scientific Services, Queensland Department of Health. Patricia Pilling, Laura Castelli, Luisa Pontes-Braz assisted with assay development.

We would also like to thank Jonneke de Rijck, Guido van der Net, Stephane Nooijen and the rest of the Viroclinics Xplore team for their work on the hamster and ferret challenge studies as well as Judith van den Brand of Utrecht University who performed the gross and histopathological examinations and analysis.

Author contribution statement

All the authors contributed to the design and/or analysis of experimental data and edited the manuscript. K.J.C., D.W., D.K.W. and N.M. wrote the initial drafts of the manuscript, and constructed the figures and tables. K.J.C., D.W., and P.R.Y. conceived the project as a component of the CEPI grant and are inventors of the molecular clamp technology. D.W and N.M performed the cryo-EM analayis. D.W. designed the Sclamp antigen panel. D.K.W. coordinated the mouse immunogenicity studies and performed the FTA analysis. T.P.M., K.J.C. and P.R.Y. directed the studies related to clinical development of Sclamp.

Conflict of interest statement

K.J.C., D.W. and P.R.Y. are inventors of the “Molecular Clamp” patent, US 2020/0040042.

References

1 Amanat, F. & Krammer, F. SARS-CoV-2 Vaccines: Status Report. *Immunity* **52**, 583-589, doi:10.1016/j.immuni.2020.03.007 (2020).

2 van Doremalen, N. *et al.* ChAdOx1 nCoV-19 vaccine prevents SARS-CoV-2 pneumonia in rhesus macaques. *Nature*, doi:10.1038/s41586-020-2608-y (2020).

3 Corbett, K. S. *et al.* Evaluation of the mRNA-1273 Vaccine against SARS-CoV-2 in Nonhuman Primates. *N Engl J Med*, doi:10.1056/NEJMoa2024671 (2020).

4 Mercado, N. B. *et al.* Single-shot Ad26 vaccine protects against SARS-CoV-2 in rhesus macaques. *Nature*, doi:10.1038/s41586-020-2607-z (2020).

5 Yu, J. *et al.* DNA vaccine protection against SARS-CoV-2 in rhesus macaques. *Science*, doi:10.1126/science.abc6284 (2020).

6 Chappell, K., Watterson, D. & Young, P. Chimeric Molecules and Uses Thereof. (2018).

7 Ekiert, D. C. *et al.* Cross-neutralization of influenza A viruses mediated by a single antibody loop. *Nature* **489**, 526-532, doi:10.1038/nature11414 (2012).

8 Huang, K., Incognito, L., Cheng, X., Ulbrandt, N. D. & Wu, H. Respiratory syncytial virus-neutralizing monoclonal antibodies motavizumab and palivizumab inhibit fusion. *J Virol* **84**, 8132-8140, doi:10.1128/JVI.02699-09 (2010).

9 (WHO), W. H. O. Novel Coronavirus (2019-nCoV) Situation Report 1. (https://www.who.int/docs/default-source/coronaviruse/situation-reports/20200121-sitrep-1-2019-ncov.pdf, 2020).

10 ter Meulen, J. *et al.* Human monoclonal antibody combination against SARS coronavirus: synergy and coverage of escape mutants. *PLoS Med* **3**, e237 (2006).

11 Wrapp, D. *et al.* Cryo-EM structure of the 2019-nCoV spike in the prefusion conformation. *Science* **367**, 1260-1263, doi:10.1126/science.abb2507 (2020).

12 Hsieh, C. L. *et al.* Structure-based Design of Prefusion-stabilized SARS-CoV-2 Spikes. *bioRxiv*, doi:10.1101/2020.05.30.125484 (2020).

13 Pinto, D. *et al.* Cross-neutralization of SARS-CoV-2 by a human monoclonal SARS-CoV antibody. *Nature* **583**, 290-295, doi:10.1038/s41586-020-2349-y (2020).

14 Hurlburt, N. K. *et al.* Structural basis for potent neutralization of SARS-CoV-2 and role of antibody affinity maturation. *bioRxiv*, doi:10.1101/2020.06.12.148692 (2020).

15 Vogel, F. R. Improving vaccine performance with adjuvants. *Clin Infect Dis* **30 Suppl 3**, S266-270, doi:10.1086/313883 (2000).

16 El Sahly, H. MF59™ as a vaccine adjuvant: a review of safety and immunogenicity. *Expert Rev Vaccines* **9**, 1135-1141, doi:10.1586/erv.10.111 (2010).

17 Tseng, C. T. *et al.* Immunization with SARS coronavirus vaccines leads to pulmonary immunopathology on challenge with the SARS virus. *PLoS One* **7**, e35421, doi:10.1371/journal.pone.0035421 (2012).

18 Knudsen, N. P. *et al.* Different human vaccine adjuvants promote distinct antigen-independent immunological signatures tailored to different pathogens. *Sci Rep* **6**, 19570, doi:10.1038/srep19570 (2016).

19 (WHO), W. H. O. 1st WHO International Standard for anti-SARS-CoV-2 antibodies. (https://www.who.int/biologicals/One_Pager_anti-SARS_CoV-2_antibodies.pdf?ua=1, 2020).

20 Ranasinghe, C., Trivedi, S., Stambas, J. & Jackson, R. J. Unique IL-13Ralpha2-based HIV-1 vaccine strategy to enhance mucosal immunity, CD8(+) T-cell avidity and protective immunity. *Mucosal Immunol* **6**, 1068-1080, doi:10.1038/mi.2013.1 (2013).

21 Wijesundara, D. K. *et al.* Use of an in vivo FTA assay to assess the magnitude, functional avidity and epitope variant cross-reactivity of T cell responses following HIV-1 recombinant poxvirus vaccination. *PLoS One* **9**, e105366, doi:10.1371/journal.pone.0105366 (2014).

22 (WHO), W. H. O. DRAFT landscape of COVID-19 candidate vaccines –

15 July 2020. (https://www.who.int/publications/m/item/draft-landscape-of-covid-19-candidate-vaccines, 2020).

23 Plotkin, S., Robinson, J. M., Cunningham, G., Iqbal, R. & Larsen, S. The complexity and cost of vaccine manufacturing - An overview. *Vaccine* **35**, 4064-4071, doi:10.1016/j.vaccine.2017.06.003 (2017).

24 Baum, A. *et al.* Antibody cocktail to SARS-CoV-2 spike protein prevents rapid mutational escape seen with individual antibodies. *Science*, doi:10.1126/science.abd0831 (2020).

25 Weiskopf, D. *et al.* Phenotype and kinetics of SARS-CoV-2-specific T cells in COVID-19 patients with acute respiratory distress syndrome. *Sci Immunol* **5**, doi:10.1126/sciimmunol.abd2071 (2020).

26 Sia, S. F. *et al.* Pathogenesis and transmission of SARS-CoV-2 in golden hamsters. *Nature* **583**, 834-838, doi:10.1038/s41586-020-2342-5 (2020).

27 Chan, J. F. *et al.* Simulation of the clinical and pathological manifestations of Coronavirus Disease 2019 (COVID-19) in golden Syrian hamster model: implications for disease pathogenesis and transmissibility. *Clin Infect Dis*, doi:10.1093/cid/ciaa325 (2020).

28 Imai, M. *et al.* Syrian hamsters as a small animal model for SARS-CoV-2 infection and countermeasure development. *Proc Natl Acad Sci U S A* **117**, 16587-16595, doi:10.1073/pnas.2009799117 (2020).

29 Huo, J. *et al.* Neutralizing nanobodies bind SARS-CoV-2 spike RBD and block interaction with ACE2. *Nat Struct Mol Biol*, doi:10.1038/s41594-020-0469-6 (2020).

30 Wang, L. *et al.* Evaluation of candidate vaccine approaches for MERS-CoV. *Nat Commun* **6**, 7712, doi:10.1038/ncomms8712 (2015).

31 Frey, G. *et al.* Distinct conformational states of HIV-1 gp41 are recognized by neutralizing and non-neutralizing antibodies. *Nat Struct Mol Biol* **17**, 1486-1491, doi:10.1038/nsmb.1950 (2010).

32 Zheng, S. Q. *et al.* MotionCor2: anisotropic correction of beam-induced motion for improved cryo-electron microscopy. *Nat Methods* **14**, 331-332 (2017).

33 Rohou, A. & Grigorieff, N. CTFFIND4: Fast and accurate defocus estimation from electron micrographs. *J Struct Biol* **192**, 216-221 (2015).

34 Scheres, S. H. A Bayesian view on cryo-EM structure determination. *J Mol Biol* **415**, 406-418, doi:10.1016/j.jmb.2011.11.010 (2012).

35 Subbarao, K. *et al.* Prior infection and passive transfer of neutralizing antibody prevent replication of severe acute respiratory syndrome coronavirus in the respiratory tract of mice. *J Virol* **78**, 3572-3577, doi:10.1128/jvi.78.7.3572-3577.2004 (2004).

36 Caly, L. *et al.* Isolation and rapid sharing of the 2019 novel coronavirus (SARS-CoV-2) from the first patient diagnosed with COVID-19 in Australia. *Med J Aust* **212**, 459-462, doi:10.5694/mja2.50569 (2020).

37 Mekonnen, Z. A. *et al.* Single-Dose Vaccination with a Hepatotropic Adeno-associated Virus Efficiently Localizes T Cell Immunity in the Liver with the Potential To Confer Rapid Protection against Hepatitis C Virus. *J Virol* **93**, doi:10.1128/JVI.00202-19 (2019).

38 Grubor-Bauk, B. *et al.* NS1 DNA vaccination protects against Zika infection through T cell-mediated immunity in immunocompetent mice. *Sci Adv* **5**, eaax2388, doi:10.1126/sciadv.aax2388 (2019).

39 (WHO), W. H. O. Guidelines on the nonclinical evaluation of vaccine adjuvants

and adjuvanted vaccines.
(https://www.who.int/biologicals/areas/vaccines/ADJUVANTS_Post_ECBS_edited_clean_Guidelines_NCE_Adjuvant_Final_17122013_WEB.pdf?ua=1, 2013).

40 OECD. *Test No. 407: Repeated Dose 28-day Oral Toxicity Study in Rodents*. (2008).

41 Walls, A. C. *et al.* Structure, Function, and Antigenicity of the SARS-CoV-2 Spike Glycoprotein. *Cell* **181**, 281-292 e286, doi:10.1016/j.cell.2020.02.058 (2020).

Methods

Constructs and plasmids

To express the prefusion S ectodomain, codon-optimised SARS-CoV-2 S (Genbank accession number: MN908947) gene with variations including (i) substitution at the furin cleavage site, (ii) substitution at signal peptide, (iii) truncation at C-terminal domain was generated with primers containing overlapping sequence by PCR mutagenesis using Phusion polymerase (New England Biolabs). These amplicons were introduced upstream of the clamp trimerisation motif. SARS-CoV-2 S RBD (aa residues 319–526) was expressed as a Fc fusion protein, which was cleaved and polished by size exclusion chromotography prior to use in downstream assays. Plasmid encoding variable domains of heavy and light chain of CR3022[10], S309[13], B38[13], H4[29], CB6[13], G4 (anti-MERS S)[30] or anti-clamp HIV1281[31] was cloned into the mammalian expression vector, pNBF-Hv or pNBF-Lv in-frame with IgK signal peptide.

Recombinant protein expression

The ExpiCHO-S expression system (ThermoFisher Scientific) was used for transient Spike protein and antibody expression. CHO cells were cultured in ExpiCHO-S Expression Medium (Gibco™) and transfection was conducted following the manufacturer's protocols for 5 or 7 days prior to harvest of the culture supernatant and protein purification. Stable cell lines were generated using the Lonza GS Xceed® System. CHOK1SV GS-KO® cells were transfected via electroporation with linearised GS expression vector encoding SARS-CoV-2 Sclamp as per manufacturer's instructions (GS Xceed® manual, Version 06 2019). Approximately 24 h later, enriched pools were selected using 50 µM L-Methionine sulfoximine (MSX) over a period of 3–4 weeks. Stable pool shaker flask expression was assessed over 12 days via Lonza's abridged fed-batch shake flask screen (v8.10) and clone selection was performed using the Beacon Optofluidic platform (Berkeley Lights). Stable pools were loaded onto the OptoSelect™ 1750b Chip as single cells. Cells were cultured on chip for 3–5 days before pens were analysed for secretion of SARS-CoV-2 Sclamp using fluorescently tagged anti-Clamp IgG. Selected pens were then exported into a 96-well plate and scaled-up into shaker flasks. Clones were further assessed via Lonza's abridged fed-batch shake flask screen (v8.10).

Recombinant protein purification

SARS-CoV-2-stabilised spike protein was purified using immunoaffinity chromatography on an ÄKTA pure protein purification system (Cytiva). This was achieved using an in-house made immunoaffinity chromatography column - the anti-clamp mAb HIV1281 coupled to 1 or 5 mL HiTrap-NHS activated HP Columns (Cytiva). CHO expression cultures were centrifuged at 4000 × g for 10 min at 4^{o}C and resultant supernatant filtered through a filter unit (0.22 µm pore size). Supernatant was added to an anti-clamp protein affinity column to purify clamp-tagged proteins or Protein A HP column (Cytvia) to purify Fc-tagged proteins and antibodies. Eluates following purification from culture supernatant were neutralised immediately and buffer-exchanged into PBS using Merck Amicon Ultra-4 or Ultra-15 centrifugal filter units. Protein concentration was determined using the NanoDrop One (ThermoFisher Scientific) or via the Pierce BCA protein assay kit (ThermoFisher Scientific). Homogeneity of purified proteins was analysed using SDS-PAGE and visualised following staining with Coomassie blue.

SE-HPLC analysis of Sclamp

High resolution assessment of the oligomeric state of Sclamp was conducted using an Agilent 1200 HPLC. Duplicate 95 µl samples were injected onto a Waters X-Bridge 300 mm column pre-calibrated with PBS mobile phase and using a flow rate of 0.8 ml/min.

Negative staining electron microscopy of pre-fusion Sclamp protein

SARS-CoV-2 proteins were diluted at ~ 10 µg/ml in PBS. Diluted proteins (4 µl) were adsorbed onto carbon-coated grids (ProSciTech) for 2 min and glow discharged for 5 sec in 25 mA. The grids were blotted and washed three times in water and stained twice with 1% Uranyl acetate with blotting in between. The grids were air dried and imaged using a Hitachi HT7700 microscope operated at 120 Kv.

Cryo-EM analysis of Sclamp

SARS-CoV-2 proteins were diluted to 0.5 mg/ml in PBS. Diluted proteins (4 µl) were adsorbed onto glow discharged quantifoil grids (Q2/1) and plunge frozen using a EMGP2 system (Leica). Grids were imaged on a CRYO ARM 300 (JEOL) equipped with a K3 detector (Gatan). 50 frame, 5 second movies were collected using JADAS software at a magnification of 50,000x, corresponding to a pixel size of 0.48 Å/pixel and a dose rate of 9e/pix/s. Movies were binned 2x during motion correction using MotionCor2 (v1.1.0)[32], giving a final pixel size of 0.96 Å. The contrast transfer function (CTF) parameters of each image were determined using CTFFIND (v. 4.1)[33]. Initial 2D references were generated using particles manually picked in RELION 3.1[34]. A 60 Å filtered map from EMD-21452 was used as an initial model for 3D classification using C1 symmetry and the most ordered class was further refined using the RELION 3D auto-refine procedure with C3 symmetry. CTF refinement and particle polishing were performed using RELION. The final half-maps were masked with a soft, extended mask and FSC calculated using the gold standard FSC cutoff of 0.143.

Thermal stability testing

Purified antigen was sterile-filtered and diluted in PBS to a final concentration of 0.18 mg/ml. 250 µl aliquots were added to 1.5 ml sterile microcentrifuge tubes which were then stored at either 4 °C, 25 °C or 40 °C for 1, 2, 4 or 8 weeks. At each designated time point, samples were removed from incubation and assessed by ELISA and SE-HPLC.

Mouse vaccinations and immune analysis

5–7 week old female BALB/c mice were purchased from the Australian Resource Centre, Perth and housed in individually ventilated HEPA-filtered cages at the University of Queensland Biological Resources facility, The Australian Institute for Bioengineering and Nanotechnology. Mice were allowed to acclimatise for at least 5 days prior to vaccination via the IM route into the hind leg muscle with 50 µl of PBS (placebo) or 5 µg/mouse of SARS-CoV-2 Sclamp with or without Alhydrogel (50 µg/mouse, InvivoGen) or MF59C.1 (50% vol:vol of SARS-CoV-2 Sclamp:MF59C.1 as recommended by the manufacturer) under anaesthesia.

Blood was collected via the tail vein prior to each vaccination and by cardiac puncture at the study end point. After overnight incubation of blood samples at 4 °C, serum was collected via centrifugation for 10 min at 10000xg, heat inactivated at 56^{o}C for 30 min and stored at -80 °C prior to analysis.

BAL collection was performed by inserting a catheter into the trachea and flushing the lungs with 400 µl of PBS. After centrifugation at 300xg for 7 min at 4 °C, clarified BAL supernatants were frozen at -80 °C prior to analysis.

To assess T cell responses in mice at the study end point, splenocyte suspensions depleted of red blood cells (RBC) were analysed using ICS or the FTA as described below.

ELISA

A capture ELISA was used to screen ExpiCHO-S supernatants and purified proteins for expression of Sclamp vaccine candidates. Nunc MaxiSorp ELISA plates were coated with 2 µg/mL of the anti-Clamp mAb HIV1281 in PBS overnight at 4˚C. Plates were then blocked with 150 µl/well of 5% KPL Milk Diluent/Blocking Solution Concentrate (SeraCare) in PBS with 0.05% Tween 20 for 1 h at room temperature (RT). Blocking buffer was removed and plates were incubated with serial dilutions of harvested ExpiCHO-S supernatant for 1 h at 37˚C. Plates were washed three times with water before incubation with 5 µg/mL of an in-house produced recombinant CR3022 mAb[10] with a mouse IgG1 backbone for 1 h at 37˚C. Following another wash step, plates were incubated with a 1:2000 dilution of a horse radish peroxidase (HRP)-conjugated goat anti-mouse secondary antibody (#A16072) for 1 h at 37˚C. After a final wash, plates were developed for 5 min using TMB Single Solution chromogen/substrate (#002023) before the reaction was stopped by addition of 2N H_2SO_4. Absorbance at 450 nm was then read on a Spectramax 190 Microplate reader (Molecular Devices).

For ELISA analysis of mouse serum from placebo- or Sclamp-immunised mice, Nunc Maxisorp ELISA plates were coated with 2 µg/ml of antigen and blocked as above. The blocked plates were incubated with serial dilutions of each mouse serum at 37 °C for 1 h. The plates were then washed, developed and read as described above. EC_{50} values were calculated by three parameter curve fitting using nonlinear regression in GraphPad Prism (version 8.3.1). The Limit of Detection (LoD) was defined as the reciprocal of the highest concentration of sera tested and any values falling below the LoD were reported as ½ LoD.

For depletion ELISA analysis of mouse serum, 10 µg/ml of the depleting antigen was added to titrated mouse serum in a 96-well round bottom plate. Antigens used for depletion included Sclamp, an alternate clamp stabilised viral glycoprotein (i.e. influenza virus haemagglutinin (HA)clamp) and SARS-CoV-2 RBD. Sera and depletion antigen were incubated at 37 °C for 1 h prior to addition to the ELISA plate and analysis as described above. The ELISA plate setup included separate rows coated with the depletion antigen as a control for incomplete depletion of domain-specific responses.

MN assay

Neutralising activity against infectious SARS-CoV-2 was assessed by a traditional MN assay as described for SARS-CoV[35]. Briefly, SARS-CoV-2 isolate CoV/Australia/VIC01/2020[36] was passaged in Vero cells and stored at -80°C. Serum samples were heat-inactivated at 56°C for 30 min and serially-diluted 1:20 to 1:10240 before addition of 100 $TCID_{50}$ of SARS-CoV-2 in MEM/0.5% BSA and incubation at RT for 1 h. Residual virus infectivity in the plasma/virus mixtures was assessed in quadruplicate wells of Vero cells incubated in serum-free media containing 1 µg/ml of TPCK trypsin at 37°C/5% CO_2; viral cytopathic effect (CPE) was read on day 5. The neutralising antibody titre was calculated using the Reed/Muench method as previously described[35]. LoD was defined as the reciprocal of the highest concentration of sera tested and any values falling below the LoD were reported as ½ LoD.

Depletion MN assay

The depletion MN assay was conducted as above with the following modifications; serum dilutions were prepared in 62.5 µl MEM in 96-well round bottom plates and mixed 1:1 with 62.5 µl of the depletion antigen (final concentration 10 µg/ml). Sera and depletion antigen were incubated at 37 °C for 1 h before addition of virus and further incubation for 1 h at RT. Each sample was then added to quadruplicate wells of Vero cells and CPE was assessed as for the standard MN assay described above.

$PRNT_{50}$ analysis

Two SARS-CoV-2 isolates generated from infected patients in Queensland, Australia were used for the PRNT assay, QLD02/2020–30/1/2020 (GISAID accession EPI_ISL_407896) and QLDID935/2020–25/03/2020 (GISAID accession EPI_ISL_436097) and were referred here as 614D and 614G, respectively. Both isolates were passaged three times in Vero E6 cells and titrated by focus-forming assay on Vero E6 cells. Serial dilutions of mouse sera and BAL were incubated with ~ 6000 focus-forming units per ml of SARS-CoV-2 for 1 h at 37 °C. Serum-virus mixtures were added to Vero E6 cell monolayers (pre-seeded at 40,000 cells/well in 96-well plates and incubated overnight) and incubated at 37 °C for 30 min. Subsequently, cells were overlaid with 1% (w/v) medium viscosity carboxymethyl cellulose in M199 (Gibco) supplemented with 2% heat-inactivated fetal bovine serum supplemented with 1% Penicillin-Streptomycin (Sigma-Aldrich) and incubated at 37°C in 5% CO_2 for 14 h. After incubation, overlay was removed and cells fixed with 80% cold-acetone in PBS for 30 min at -20 °C. Plates were then dried, blocked with blocking buffer (1xKPL in 0.1% PBS-Tween 20) for 1 h and then incubated with 1 µg/ml of CR3022 anti-S mAb and 0.2 µg/ml IR-Dye800-conjugated goat anti-human IgG (LI-COR) in blocking buffer. Plates were washed 3 times after antibody incubations by submerging in PBS with 0.1% Tween-20. Plates were then dried prior to visualising using Odyssey (LI-COR). Immunoplaques were manually counted in blinded fashion.

FTA analysis

FTA analysis was performed using a well-established method as previously described[37,38]. In brief, naïve autologous BALB/c splenocytes were evenly split and serially labelled with 0.12, 0.46, 1.7, 6.2, 23 or 85 µM of CTV (Invitrogen) and 10 or 39 µM of CPD (Invitrogen) for 5 min at RT. Each of the dye-labelled populations was pulsed with DMSO (nil) or 10 µg/ml/peptide of the indicated peptide pools comprising of 15–18 aa peptides (10–11 aa overlap between adjacent peptides) for 4 h at 37 °C with 5% CO_2. Overlapping peptides spanning the SARS-CoV-2 S_{1-1226} and the Peptivator array ($S_{304-338}$, $S_{421-475}$, $S_{492-519}$, $S_{683-707}$, $S_{741-770}$, $S_{785-802}$ and $S_{885-1273}$) used for peptide pulsing were purchased from Shanghai RoyoBiotech and Miltenyi Biotec, respectively. The FTA was then injected intravenous into placebo or vaccinated mice such that each mouse received 24×10^6 cells (2×10^6 cells from each fluorescent bar-coded target cell population) in 200 µl of PBS.

Fifteen hours after the injection, RBC-depleted splenocytes from FTA-challenged mice were stained with PE-Cy7 conjugated anti-mouse CD69 (clone H1.2F3, BD Biosciences) and BUV395 conjugated anti-mouse B220 (clone RA3-6B2, BD Biosciences) and fixed using 0.5% paraformaldehyde. Subsequently, stained samples were acquired using the BD LSRII and analysed using the FlowJo software (version 8.8.7). GMFI of CD69 plotted was calculated using the formula: $B220^+$ peptides-pulsed target value (GMFI of CD69) - $B220^+$ nil target value (GMFI of CD69). The following formula was used to calculate the % killed data: [(nil target value % - peptides-pulsed target value %)/nil target value %] x 100.

ICS analysis

2×10^6 RBC-depleted splenocytes from vaccinated or placebo control mice were seeded into wells of a 96-well round-bottom plate and stimulated with 5 µg/ml of S_{1-1226} at 37 °C with 5% CO_2 for 12 h. DMSO and PMA/Ionomycin (PMA at 25 ng/ml and Ionomycin at 1 µg/ml) stimulations were included as negative and positive controls, respectively. Following the 12 h incubation, 1 µg/ml of brefeldin-A (BioLegend) was added to each well and incubated for further 4 h prior to staining the cells with fluorochromeconjugated monoclonal antibodies. The stimulated cells were stained for cell-surface markers, fixed and permeabilised using IC Fix/Perm buffer (BioLegend) prior to the intracellular stain to analyse cytokine expression. The following fluorochrome-conjugated monoclonal antibodies were used to stain the cells: CD3 (clone: 17A2, BioLegend), CD4 (clone: GK1.5, BioLegend), CD8 (clone: 53 – 6.7, BioLegend), IFN-γ (clone: XMG1.2, BioLegend), TNF-α (clone: MP6-XT22,

BioLegend), IL-2 (clone: JES6-5H4, BioLegend), IL-4 (clone: 11B11, BioLegend) and IL-13 (clone: eBio13A, eBioscience). Stained cells were acquired using the BD LSRII flow cytometer and analysed using the FlowJo software (version 10.8).

Preparation of formalin-inactivated virus

To prepare formalin-inactivated virus, SARS-CoV-2 was cultured in Vero E6 cells for 3 days before harvesting supernatant and clarification via centrifugation. Formalin was added to the virus stock at 1:4000 and incubated at 37 °C for 3 days. The formalin-treated virus stock was centrifuged using Millipore Amicon filters to concentrate the virus prior to removal of formalin and buffer-exchange using PBS. Virus was passaged on Vero E6 cells to confirm loss of infectivity. Virus protein concentration was quantified by BCA analysis.

Safety and toxicology

A repeat dose toxicity study was conducted in Sprague Dawley rats in accordance with current guidelines[39,40]. Three IM doses of either saline or 20 µg SARS-CoV-2 Sclamp in a 200 µl bolus with or without MF59C.1 adjuvant were administered to adult rats at fortnightly intervals over a four-week period. This dose level corresponds to 40% of the intended maximum clinical dose of 50 µg of SARS-CoV-2 Sclamp antigen. At 24–48 h following administration of the final dose, terminal examinations were conducted on ten rats per sex from each treatment group. Five additional rats per sex, from each group were allowed a treatment-free recovery period of a further two weeks prior to necropsy. Animals were observed daily over the course of the study for changes in skin and fur, eyes and mucous membranes, respiratory and circulatory function, gait and posture, behaviour, tremors or convulsions and any other abnormal findings. These observations also included daily examination of the injection site for reactions (oedema, erythema and eschar). Upon sacrifice, terminal blood samples were collected for haematology, coagulation, biochemistry and SARS-CoV-2 IgG antibody titre assessments. Necropsy procedures included a detailed examination of the external appearance of the animal and internal organs, weights of critical organs, and collection and preservation of the tissues and organs. All tissues and gross lesions were subjected to microscopic examination.

Hamster challenge study

Syrian hamsters (n = 10 per group) were vaccinated with either a single dose or two doses as shown in Fig. 4A and 4B. Vaccination with PBS alone was used as a placebo and vaccination with 50 µg of formalin-inactivated SARS-CoV-2 virus formulated with Alhydrogel was included as a comparator vaccination. All vaccines were delivered by IM immunisation. For formalin-inactivated SARS-CoV-2 + Alhydrogel vaccination 100 µl total volume was delivered per dose, while all other vaccines comprised a total volume of 50 µl per dose. For an infection and recovery comparator group, hamsters were housed separately in a BSL-3 containment isolator and infected with 10^2 $TCID_{50}$ of SARS-CoV-2 (BetaCoV/Munich/BavPat1/2020) diluted in PBS to a dose volume of 100 µl delivered via IN administration.

At 4 weeks after the single dose or prime/boost vaccination, or 7 weeks after infection in the infection and recovery group, hamsters were challenged with 10^2 $TCID_{50}$ of SARS-CoV-2 (BetaCoV/Munich/BavPat1/2020) diluted in PBS to a dose volume of 100 µl delivered via IN administration. Following challenge, animal weight loss was recorded daily and throat swabs taken for virus quantification by $TCID_{50}$ and qPCR. At the time of peak (day 4) or resolution (day 8) of infection, animals were sacrificed and tissue samples collected from the lung lobes and nasal turbinate to measure virus titre by $TCID_{50}$ and qPCR. Samples were also fixed and sectioned to enable the assessment of lesions by gross pathology as well as histopathological assessment for evidence of congestion, emphysema, presence of foreign body, alveolar hemorrhage, bronchioloalveolar hyperplasia and inflammation and edema.

Ferret challenge study

Ferrets (n = 5 per group) were vaccinated with a single IM dose containing 20 µg of SARS-CoV-2 Sclamp in a 200 µl bolus of MF59C.1. Vaccination with PBS alone was used as a placebo and vaccination with 50 µg of formalin-inactivated SARS-CoV-2 virus formulated with Alhydrogel was included as a comparator vaccination. At 4 weeks after dosing ferrets were infected IN with 10^6 $TCID_{50}$ of SARS-CoV-2 (BetaCoV/Munich/BavPat1/2020) diluted in 300 µl of PBS. Following challenge, animal weight loss was recorded daily and nose and throat swabs taken for virus quantification by $TCID_{50}$ and qPCR. At 4 days post-challenge animals were sacrificed and the lung lobes and nasal turbinate samples collected to measure virus titre by $TCID_{50}$ and qPCR. Samples were also fixed and sectioned to enable the assessment of lesions by gross pathology as well as histopathological analysis as described above.

Statistical analysis

Statistical analysis of the data was performed using the IBM SPSS Statistics Software (version 25) or GraphPad Prism (version 8.3.1). P values are reported for statistically significant comparisons with $p < 0.05$. Non-significant data with $p > 0.05$ are denoted ‘ns’.

Figures

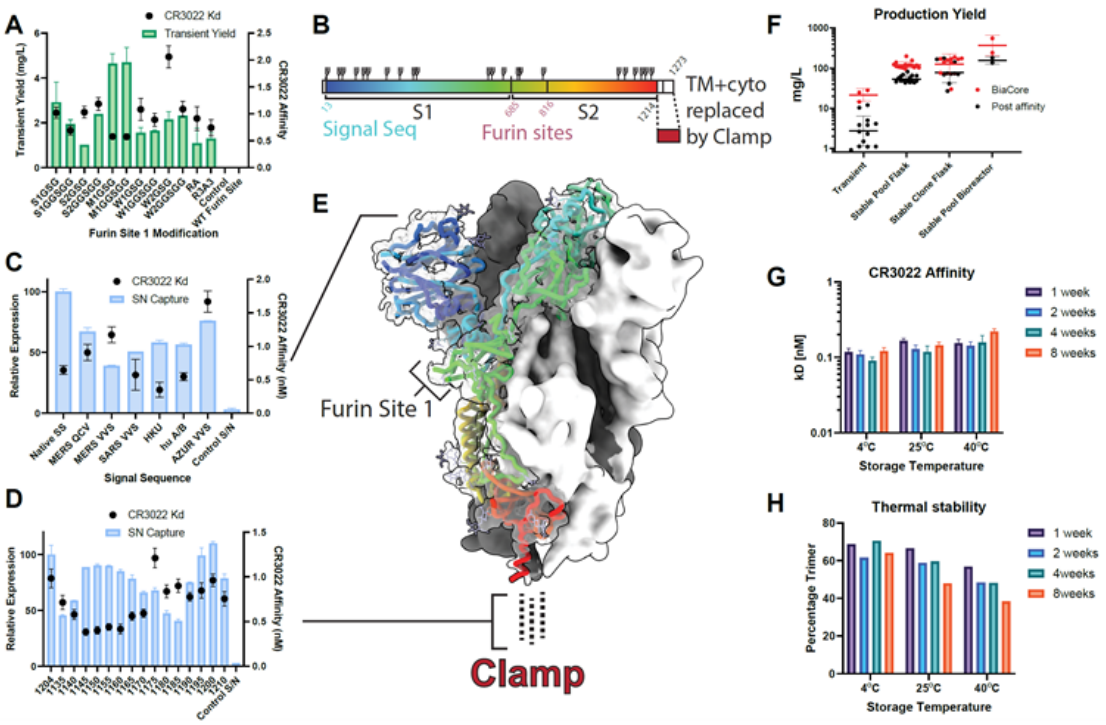

Figure 1

Antigen design and analysis. A, In vitro screening of S1/S2 linker modifications for yield and CR3022 affinity (KD). B, Linear representation of recombinant spike antigen, C, In vitro screening of signal sequence changes yield and CR3022 affinity (KD) D, In vitro screening of C-terminal length for yield and CR3022 affinity. E, Cryo-TEM reconstruction of antigen structure, fitted with prefusion Spike structure PDB:6VXX41 shown in rainbow cartoon for one S monomer. F, Production yield from CHO cell culture transient expression, stable pools and clones in flasks or bioreactors. Red - antigen concentration in cell culture supernatant estimated by BiaCore. Black - Protein recovery following immunoaffinity purification measured by absorbance at 280 nm. G, Stability of stable pool derived Sclamp as assessed by CR3022 affinity (KD) following incubation at 4°C, 25°C, or 40°C for up to 8 weeks. H, Stability of stable pool derived Sclamp as assessed by percentage trimer analysis using SE-HPLC following incubation of the protein at 4°C, 25°C, or 40°C for up to 8 weeks.

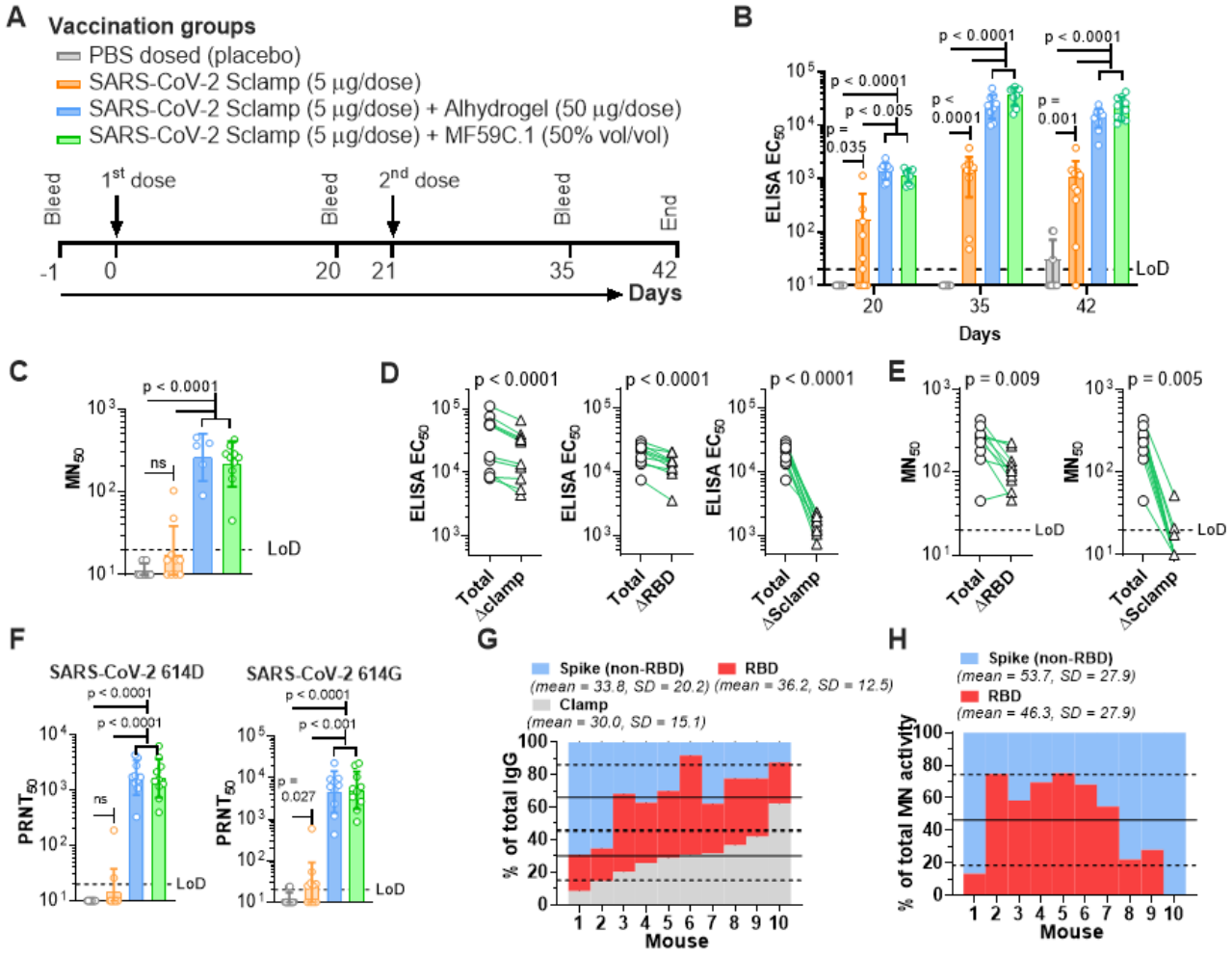

Figure 2

The antibody response following SARS-CoV-2 Sclamp vaccination in BALB/c mice. A, Prime/boost vaccination and bleed schedule for the study. B, SARS-CoV-2 Sclamp-specific IgG EC50 titre (reciprocal EC50) in vaccinated mice 20-, 35- and 42-days following intramuscular injection of the first dose. C, MN titre against infectious SARS-CoV-2 (614D). D, Analysis of clamp-specific, RBD-specific and non-RBD S-specific IgG EC50 titre assessed by depletion ELISA. Each line represents the response from a single mouse. E, Analysis of RBD-specific and non-RBD S-specific MN titre against infectious SARS-CoV-2 (614D) evaluated using the depletion MN assay, as described in Methods. Each line represents the response from a single mouse. F, MN titre against SARS-CoV-2 614D and 614G isolates evaluated by PRNT50 assay. G, Relative percentage of total IgG response directed to the clamp domain, RBD and non-RBD spike epitopes, calculated based on EC50 titres in D. H, Relative percentage of MN titre directed to the RBD and non-RBD spike epitopes, calculated based on titres in E. Analysis for panels C-H was limited to day 42 sera from Ag + MF59C.1 vaccinated mice only. P values were calculated using: 1) one-way ANOVA with Tukey's multiple comparison post-hoc test for normally distributed and homoscedastic data, 2) Welch's ANOVA with Games-Howell post-hoc analysis for all heteroscedastic data and 3) Pairwise Kruskal-Wallis H test for non-normally distributed and homoscedastic data sets.

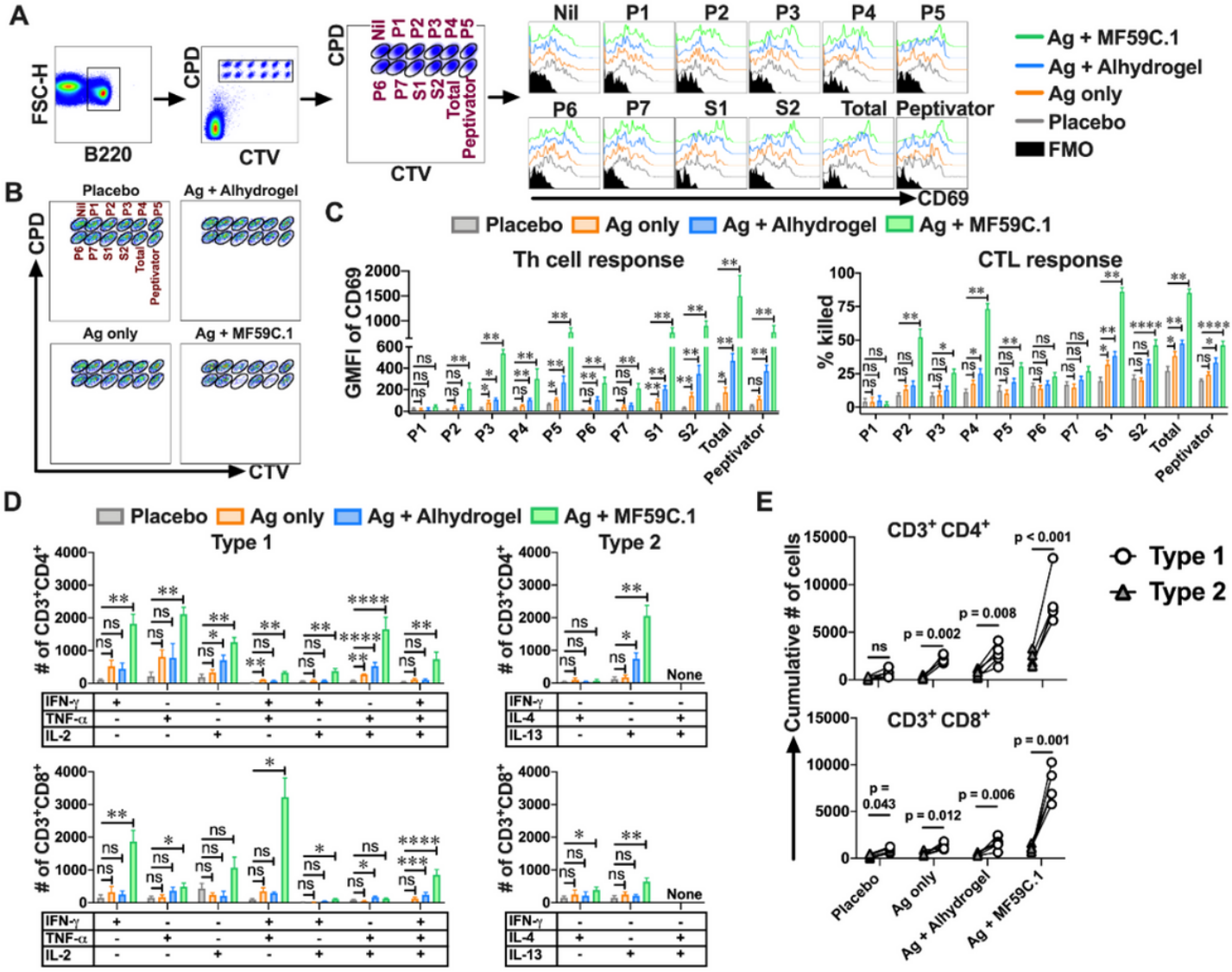

Figure 3

MF59C.1-adjuvanted SARS-CoV-2 Sclamp vaccination elicits potent T cell responses in mice. A, Representative flow cytometry plots show the gating strategy for analysis of S-specific Th cell responses based on the up-regulation of CD69 on peptide-pulsed B220+ single cells in the FTA. BALB/c mice vaccinated as in Figure 2A were challenged 19 days after boost with the FTA comprising S peptide-pulsed, cell proliferation dye (CPD) and cell trace violet (CTV)-labelled targets. B, Dot plots showing all targets recovered from a representative FTA-challenged mouse which were used to analyse the S-specific CTL responses as described in Methods. C, Bar graphs show the mean (n = 5) and SEM of the geometric mean fluorescent intensity (GMFI) of CD69 on gated B220+ cells and the percentage of peptide-pulsed targets that were killed in the FTA. D, Mean (n = 5) and SEM of the number of the indicated cytokine-producing S1-1226-specific CD4+ or CD8+ T cells. E, Cumulative number of type 1 or type 2 cells in individual mice from the analysis in D. Each line represents an individual mouse response. For the ICS analysis, splenocytes recovered 24 days following boost from mice prime/boost vaccinated at 2-weekly intervals were stimulated for 16 h with the Total pool. For C and D, p values for all the comparisons are shown in Supplementary Tables 2-5 and the p values shown indicate significance relative to placebo (* = $p < 0.05$; ** = $p < 0.01$; *** = $p < 0.001$; **** = $p < 0.0001$). For the paired data exhibiting a normal or non-normal distribution a paired t-test or Wilcoxon Signed-Rank test was used to calculate the p values respectively.

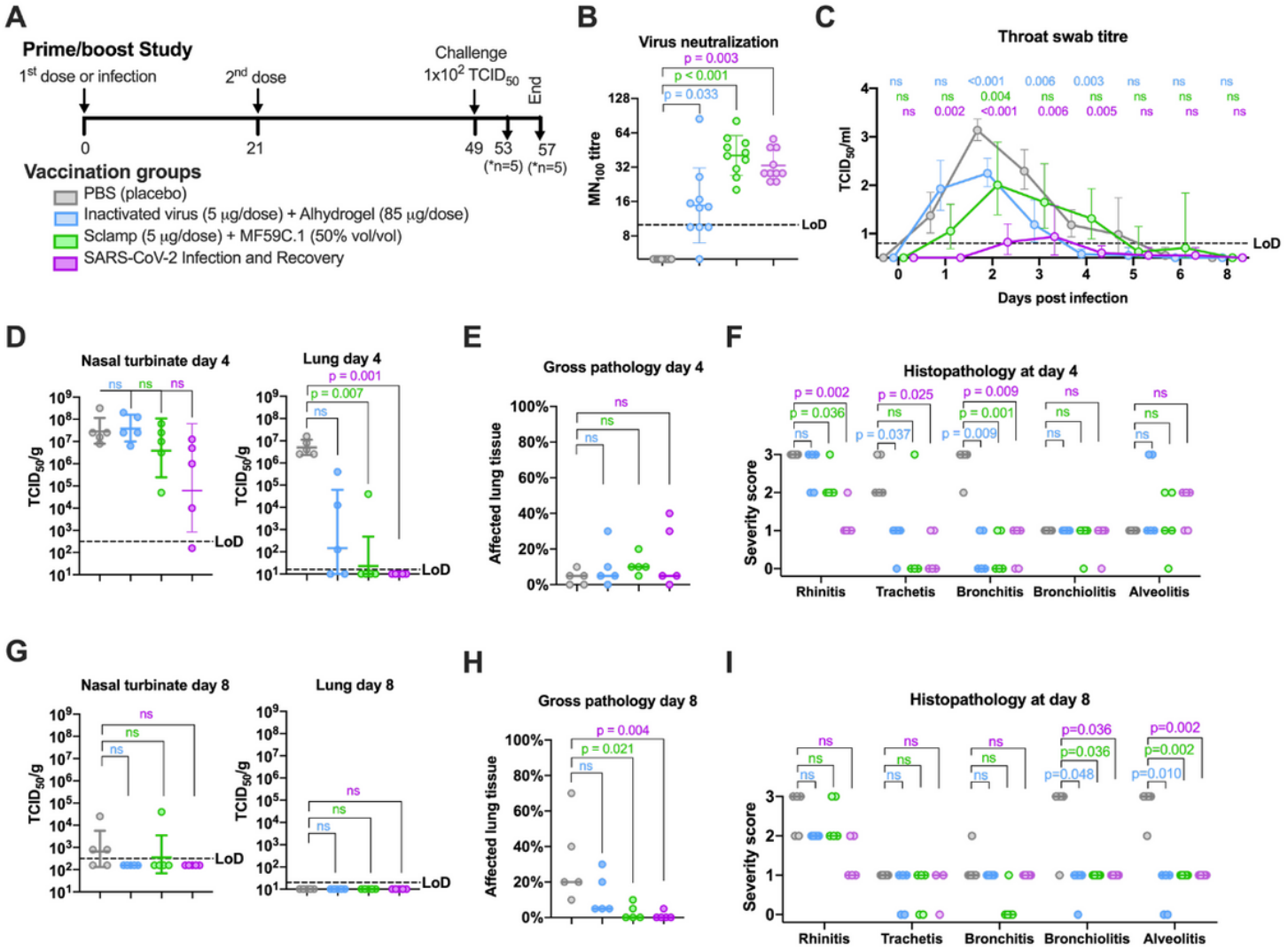

Figure 4

Hamster two dose protection study. A) Prime/boost study schedule. B) SARS-CoV-2 MN titre was measured for hamster serum collected at day 42 and 49 and the average MN100 titre graphed C) Virus quantification in daily throat swabs taken post-infection. D/G) Viral loads in nasal turbinates and lung tissue at day 4 and day 8 post-infection. E/H) Extent of affected lung tissue damage assessed by gross pathology at day 4 and day 8 post-infection. F/I) Severity score of inflammatory response based on histology at day 4 and day 8 post-infection; 0 = no inflammatory cells, 1= few inflammatory cells, 2 = moderate number of inflammatory cells and 3 = many inflammatory cells. P values were calculated using a Kruskal-Wallis ANOVA with Dunn's multiple comparison tests or a Two-Way ANOVA with Dunnett's multiple comparison tests.

Supplementary Files

This is a list of supplementary files associated with this preprint. Click to download.

- SupplementaryFigures16092020.docx
- SupplementaryTables16092020.docx
- Extendeddatafiles1692020.docx